Influence of annealing on the hydrogen bonding and the microstructure of diamondlike and polymerlike hydrogenated amorphous carbon films

Y. Bounouh and M. L. Thèye
Laboratoire d'Optique des Solides, URA CNRS 0781, Université Pierre et Marie Curie, Case 80, 75252 Paris Cédex 05, France

A. Dehbi-Alaoui and A. Matthews
Research Center in Surface Engineering, University of Hull, Hull HU6 7RX, United Kingdom

J. P. Stoquert
Groupe PHASE, Centre de Recherches Nucléaires, Boîte Postale 20, 67037 Strasbourg Cédex, France
(Received 3 August 1994; revised manuscript received 13 December 1994)

The influence of hydrogen incorporation on the microstructure of hydrogenated amorphous carbon (*a*-C:H) films has been studied in detail by applying several complementary methods, i.e., elastic recoil detection analysis (ERDA), hydrogen evolution, and infrared absorption measurements, to two series of samples prepared by two different techniques, respectively representative of diamondlike and polymerlike *a*-C:H. The analysis of the changes of the infrared vibrational spectra over a large frequency range upon annealing at increasing temperatures up to 600 °C allowed us to get insights into both the C—H and C—C bonding modifications.

I. INTRODUCTION

Although hydrogen incorporation strongly affects the microstructure as well as the electronic properties of both hydrogenated amorphous silicon (*a*-Si:H) and hydrogenated amorphous carbon (*a*-C:H), its role is significantly different in the two materials. In the *a*-Si:H case, hydrogen essentially saturates part of the dangling bonds, which results in the removal of the corresponding localized states from the pseudogap, and its effects on the amorphous silicon network itself are comparatively of minor importance. In the case of *a*-C:H prepared by decomposition of hydrocarbons on the contrary, the hydrogen influence is far more determinant and complex. By bonding preferentially to sp^3 or sp^2-hybridized carbon sites, it seems to control not only the sp^3 or sp^2 C ratio, but also the morphology of the deposit, which in turn determines the electron state density to a large extent.[1,2] It is, therefore, very important to understand how the hydrogen incorporation, the material microstructure, and its electronic properties are linked together. In the present paper, we investigate such correlations in two series of well-characterized *a*-C:H samples, which were intentionally chosen because of the large differences between their properties, due to two different methods of preparation. We concentrate here on the analysis of the infrared vibrational spectroscopy results over a large frequency range, and on their modifications upon annealing cycles at increasing temperatures up to 600 °C. These data are correlated with the simultaneous changes in the electronic optical properties.

II. EXPERIMENT

The samples were thin films, 0.5–2 μm thick, deposited by two completely different techniques to ensure quite different material microstructures.[3] Series I was prepared by direct vapor deposition from a low-pressure cold cathode device (Fast Atom Beam Source) supposed to give mainly neutral species, with butane as the source gas, on unbiased substrates. The deposition rate was low ($\sim$300 nm/h) and the substrate temperature remained close to room temperature ($<$50 °C). These films had a low optical gap and were extremely hard [2000–8000 H_K (25 g)], with some elastic recovery. They can be considered as diamondlike samples. Series II was obtained by electron gun evaporation of graphite in a butane plasma, a dc bias being directly applied to the substrates; the low-pressure discharge had to be sustained by a negatively biased filament. The deposition rate was much higher ($\sim$3 μm/h) and the substrate temperature increased up to $\sim$350 °C during deposition. The energy of the impinging ions could be changed by varying the substrate bias. These films had a larger optical gap and were brittle, with poor adhesion to the substrate. They can be considered as polymerlike samples.

The film thickness d was determined on films deposited on Corning 7059 glass substrates from the analysis of the interference fringes of the optical transmission spectra in the near infrared (which also yielded the values of the refractive index n), and measured directly on films deposited on glass and crystalline Si substrates with a Tenkor P.1 profilometer. The results of the two techniques agreed within experimental uncertainties ($\sim$5%).

The total H atomic concentration, as well as its profile over a $\sim$300-nm depth from the surface, were obtained from elastic recoil detection analysis (ERDA) experiments, performed with ^{4}He nuclei with an energy of 2.9 MeV, at angles $\alpha=\beta=10°$. We checked that the results obtained for films deposited simultaneously on Corning glass 7059 and crystalline silicon substrates were identical, even if the film thicknesses were different; this was

especially important for series II where the properties can vary with the substrate bias.

H evolution experiments were performed on a few samples of the two series deposited on crystalline Si substrates, in a quartz tube with a base pressure of 10^{-9} Torr, at a constant heating rate of 10 °C/min. We explored the masses up to $M=17$, and we followed the signals for H_2^+, corresponding to H_2 evolution, and CH_2^+, CH_3^+, CH_4^+, corresponding to CH_4 evolution.

The infrared transmission experiments were performed with a Perkin Elmer 580 B conventional double-beam spectrophotometer, on films deposited on 500-μm-thick crystalline Si substrates with both faces polished. An identical bare substrate was put on the reference beam in order to compensate for absorption in the Si substrate. The observation of a positive peak corresponding to SiO_2 absorption in the series II transmission spectra indicated that, in this case, the oxide surface layer of the sample substrate was probably removed by ion bombardment prior to deposition. The transmission spectra presented interference fringes, which were eliminated by fitting the corresponding background, outside the absorption bands, according to the approximate transmission expression: $T(\lambda)=e^{-\alpha d}[A+B\cos(C/\lambda)]^{-1}$. Uncertainties due to this procedure, as well as bad signal-to-noise ratio, renders the α determination less reliable below 1000 cm^{-1}, but qualitative information could still be obtained down to 500 cm^{-1}. No attempt at deriving quantitative information on the bonded H concentration was made in the absence of well-established values of the oscillator strengths for the different CH_x configurations.

The experiments were performed both on the as-deposited samples, and on the same samples after successive annealing cycles at increasing temperatures up to $T_A=600$ °C, under a pressure of $\sim 10^{-7}$ Torr. The heating rate was 2°C/min, and the samples were maintained at T_A for 2 h in each cycle. The film thickness and refractive index were measured again after annealing. It must be emphasized that one must take into account the difference in the thermal kinetics during such annealing cycles and during H evolution experiments, when comparing the results of the two techniques.

III. SAMPLE CHARACTERIZATION

The total H atomic concentration as measured by ERDA is of the order of 25 at. % for all series I films, of the order of 50 at. % for the series II films, with, however, a dispersion of ±5 at. %, which does not correlate with the substrate bias. Figures 1(a) and 1(b) show typical examples of the total H content (expressed as the H/C ratio) profile given by ERDA for series I and series II films. These profiles are rather flat, with, however, a slight decay towards the surface. Upon annealing, they remain flat up to $T_A=500$ °C. For $T_A=600$ °C, Figs. 2(a) and 2(b) show that there is a H deficit close to the surface in series I, while on the contrary the H content decreases towards the interface with the substrate in series II. This is a first indication of different H incorporation.

Typical H evolution spectra are presented in Figs. 3(a) and 3(b) for series I and II, respectively; they are strikingly different. In series I samples, the evolving gas is mainly hydrogen, with only a small contribution from methane CH_4. The H_2 and CH_4 spectra have essentially the same shape, with a very slow start at low temperatures, a low plateau above ~400 °C, and a steep increase at about 500 °C, with a maximum at about 600 °C in both cases. However, while the CH_4 evolution goes to zero at about 700 °C, the H_2 one starts to increase again at that temperature. Such a behavior suggests a rather dense material,[4,5] with, however, a non-negligible concentration of CH_x groups besides CH groups. In series II on the contrary, the evolving gas is mainly CH_4, with, however, a significant H_2 contribution. Again one first observes a plateau (up to 400 °C) but the evolution begins at lower temperatures than in series I (~150–200 °C). Then both H_2 and CH_4 start to evolve rapidly until about the same temperature, of the order of 530 °C. Here also the H_2 evolution increases again at high temperatures (above 600 °C), while the CH_4 one goes towards zero. These results indicate a more porous material,[4,5] and a large proportion of polyhydride groups. The porosity is confirmed by the presence of bulk contamination by oxygen and nitrogen, clearly evidenced by the IR absorption data.

The optical properties of series I samples are almost insensitive to the deposition parameters [anode potential in

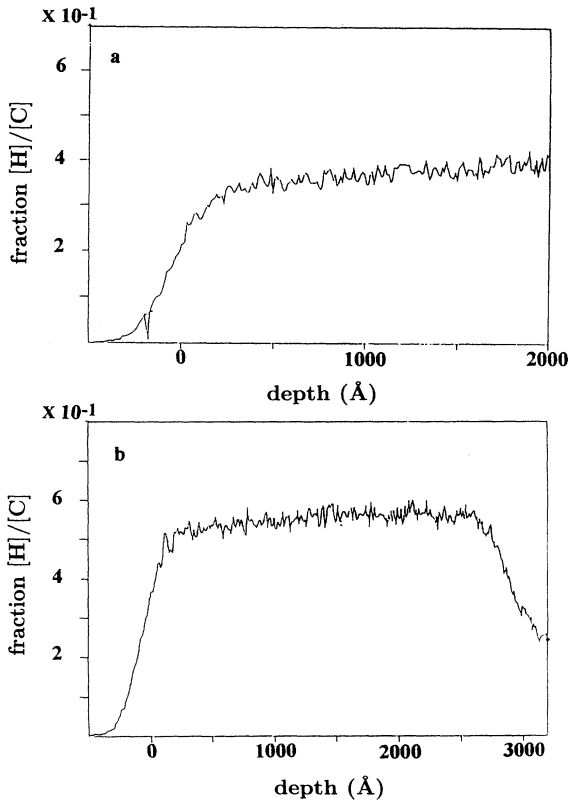

FIG. 1. Total H distribution profile vs probed depth for typical as-deposited *a*-C:H films of series I (a) and series II (b).

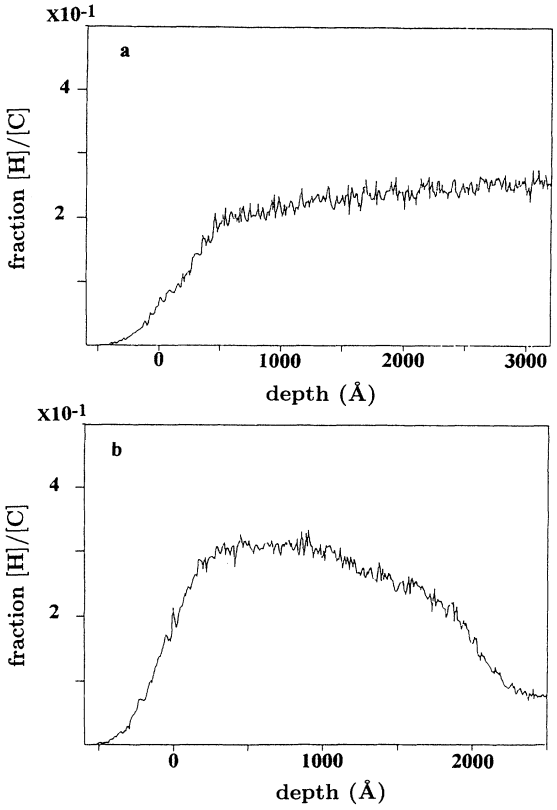

FIG. 2. Total H distribution profile vs probed depth for typical *a*-C:H films of series I (a) and II (b) after annealing at $T_A = 600\,^{\circ}C$.

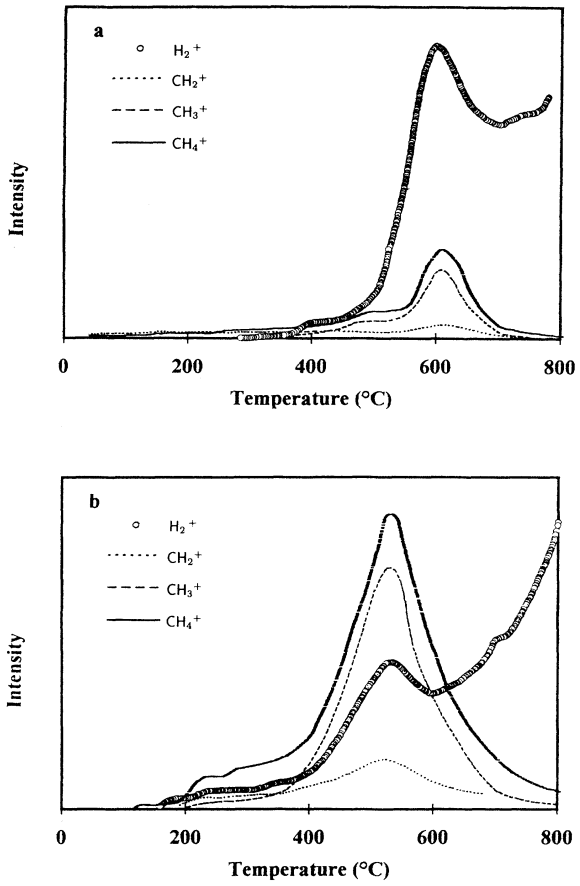

FIG. 3. Hydrogen evolution spectra for series I (a) and series II (b) samples.

the Fast Atom Beam source, gas flux]. The refractive index at 2 μm, n_0, is of the order 2.3–2.5, which is quite high for *a*-C:H; the optical gap E_{04} (i.e., the energy at which the absorption coefficient is equal to $10^4\ cm^{-1}$) is always between 1.2 and 1.3 eV. On the contrary, the properties of series II samples vary with the bias V_c applied to the substrate, as expected since this parameter determines the energy of the impinging ions during deposition.[6] If n_0 remains equal to 1.6–1.7, which is much lower than the series I values, E_{04} decreases with increasing V_c: from 3.3 eV for $V_c = 100$ V to 2.8 eV for $V_c = 600$ V. There is no clear correlation between E_{04} and the total H content. We are more interested here in the variations of the optical parameters upon annealing, which are presented in Table I for two typical samples of series I and II. It can be seen that annealing at $T_A = 300\,^{\circ}C$ has practically no effect for both series, except for the gap of the series II film, which decreases significantly without any corresponding change in n_0 and/or d. Annealing at higher T_A produces a gradual decrease of the thickness d, an increase of the refractive index n_0, and a decrease of the optical gap, which is much more important in series II. We will come back to these data in the following discussions.

TABLE I. Values of the thickness d, the refractive index at 2-μm n_0, and the optical gap E_{04}, for two typical films of series I ($x_H = 0.26$) and series II ($x_H = 0.44$), as-deposited and after annealing at increasing T_A.

	Series I			Series II		
T_A	d (μm)	n_0	E_{04} (eV)	d (μm)	n_0	E_{04} (eV)
As-dep	0.840	2.34	1.33	1.206	1.70	3.30
300	0.806	2.37	1.33	1.211	1.66	2.76
400				0.819	2.05	2.20
500	0.470	3.31	0.98	0.603	2.10	1.37

IV. INFRARED ABSORPTION SPECTRA

A. As-deposited samples

The optical-absorption spectra obtained over the whole infrared range investigated (4000–500 cm^{-1}) for typical samples of series I and II are compared in Fig. 4. One clearly distinguishes two main absorption bands. The high-frequency band around 2900 cm^{-1} is due to the stretching vibrations of the C—H bond in its different configurations, while the low-frequency one below 1800 cm^{-1}, which is much wider and presents well-defined structures, has a more complex origin, as we will discuss below. The additional bands observed for the series II samples around 3400 and 1700 cm^{-1} are due to bulk contamination by ambient atmosphere (which does not exist for series I samples) and are attributed to vibrations of the OH and C=O, C=N groups, respectively. Such a contamination indicates an open porous microstructure, which is consistent with the particularly low values of the refractive index n_o. The impurity bands decrease gradually upon annealing, and disappear completely for $T_A = 500\,°C$.

The C—H stretching bands are compared in more detail in Fig. 5. These spectra are, respectively, typical of each series. Their line shape remains the same for all samples in one series, even if their intensity may vary somewhat with deposition conditions in series II. It can immediately be seen that the concentration of bonded H is much larger in series II than in series I, the ratio of the total band areas being of the order of 4 (Table II). This has to be compared with the values of the total H concentration as deduced from ERDA experiments, the ratio of which is only of the order of 2. Such a discrepancy is surprising, since the presence of unbonded H (Ref. 7), which could explain a lack of consistency between the IR and ERDA results, is expected in series II rather than in series I. Our data then suggest possible differences in the oscillator strengths of the various sp^3 CH_x and sp^2 CH_x groups present in different proportions in the two series of samples.

Although the assignments of the high-frequency stretching modes are well established,[6,8] it is important to determine the respective contributions of the different possible C—H configurations. From extensive studies of hydrocarbons,[9,10] it is well known that the stretching (and the bending) sp^3 C—H vibrations in methyl (CH_3) and methylene (CH_2) groups are rather insensitive to their environment, both in frequency and in IR absorption intensity. Although such conclusions strictly apply to unstrained hydrocarbons in which these groups are only linked to other C atoms, they are likely to remain valid, to a certain extent, in the case of *a*-C:H.[8] The subpeak at 2870 cm^{-1} and the shoulder at 2960 cm^{-1}, which are clearly observed in series II, can then be attributed to in-phase (symmetric) and out-of-phase (antisymmetric) CH_3 stretching vibrations. In the same way, the maximum at 2925 cm^{-1} can be ascribed to out-of-phase CH_2 stretching vibrations; the corresponding in-phase CH_2 vibrations are certainly responsible for the tailing of the band towards low frequencies. This indicates large proportions of CH_2 and CH_3 groups in series II, which is consistent with the "polymeric" character of these samples. One may also expect a faint contribution from the stretching vibrations of CH groups around 1915 cm^{-1}. The series II stretching band below 3000 cm^{-1} can indeed be easily decomposed into five Gaussian components centered on these frequencies, as shown in Fig. 5(b). The only ambiguity concerns the respective strengths of the 2915- and 2925-cm^{-1} components because of their strong frequency overlap; but, when leaving all parameters free in the fitting procedure, the latter is always much more intense than the former (by a factor

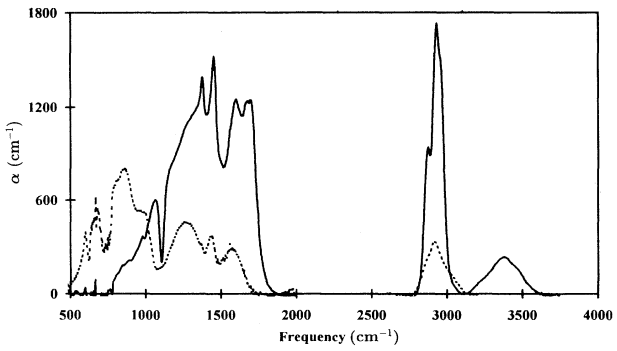

FIG. 4. Comparison of the infrared absorption spectra obtained for as-deposited series I (dashed line) and series II (continuous line) samples from 4000 to 500 cm^{-1}.

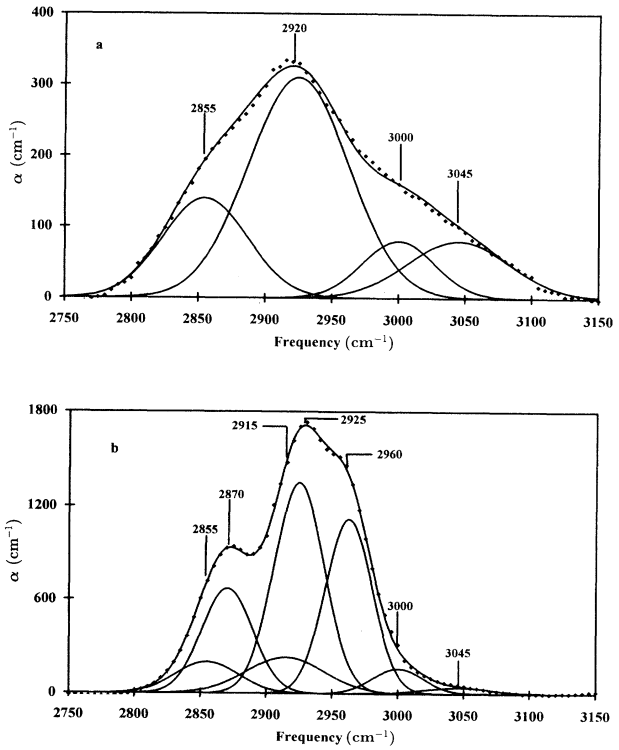

FIG. 5. Decomposition of the high-frequency C—H stretching bands of the IR absorption spectra into Gaussian components for as-deposited series I (a) and series II (b) samples.

TABLE II. Values of the areas under the total stretching band and under the components of this band ascribed to sp^3 CH_x and sp^2 CH_x stretching vibrations for the same *a*-C:H samples as in Table I.

	Series I			Series II		
T_A (°C)	Total	sp^3	sp^2	Total	sp^3	sp^2
As-dep	54	40	13	185	175	10
300	57	39	18	167	155.5	11.5
500	49.5	34.5	15	8.5	0	8.5
600	19.5	0	19.5	8	0	7.8

of 3.5–4). A decomposition along the same lines proves to be more difficult for series I because of the lack of well-defined structures in the absorption band (which is a common feature of all diamondlike films). It appears, however, that the stretching band is in this case dominated by the contributions of CH_2 and CH groups, with a much smaller participation of CH_3 groups. In fact, the band below 3000 cm^{-1} can as well be reproduced by using only two Gaussian components centered at 2920 and 2855 cm^{-1}, respectively, as shown in Fig. 5(a).

Differences between series I and II also appear in the high-frequency range of the stretching band. For series I, the data are well reproduced by two Gaussian components centered at 3000 and 3045 cm^{-1}, with comparable intensities [Fig. 5(a)], which may be ascribed to stretching vibrations of olefinic and aromatic sp^2 CH groups, respectively.[8] For series II, the presence of the nearby contamination band makes the subtraction of the background more difficult. The tailing of the stretching band towards high frequencies, which is nevertheless observed, cannot just be attributed to broadening effects, and an olefinic contribution is definitely observed at 3000 cm^{-1} [Fig. 5(b)]. The aromatic contribution, if present, is certainly very small.

Complementary information can be gained from the analysis of the IR absorption spectra below 1800 cm^{-1}. This region has comparatively received less attention and, although several experimental spectra were reported in the literature,[11–19] the assignments of the different features are still uncertain.[2,6,20] In the following, we will rely heavily on the hydrocarbon data,[9,10] and confirm our interpretations by following the changes of the main structures upon annealing.

The low-frequency IR absorption bands of our as-deposited series I and series II samples are compared in Fig. 6(a); the sharp minimum centered at 1105 cm^{-1} in all series II spectra is an artifact coming from substrate effects—due to the SiO_2 surface layer—which could not be compensated for in this case, as explained in the experimental section.

The most prominent feature in the series-II spectrum is the sharp doublet centered at 1455–1375 cm^{-1}. It can without ambiguity be ascribed essentially to out-of-phase ($\sim$1450 cm^{-1}) and in-phase ($\sim$1375 cm^{-1}) deformation vibrations of the sp^3 CH_3 groups, which are known to give rise to good group frequencies like the stretching vibrations of the same groups; the 1375-cm^{-1} component can even be considered as a signature of the presence of methyl groups.[9,10] This is consistent with the presence of well-defined features at 2870 and 2960 cm^{-1} in the stretching band, which are also characteristic of methyl groups. On the contrary, the 1455–1375-cm^{-1} doublet is absent in the series-I spectrum, again in agreement with our conclusions from the analysis of the stretching band. We rather observe in this case a broader but still well-defined peak centered at about 1430 cm^{-1}, and only a faint structure around 1370 cm^{-1}, which can hardly be detected over the background. The 1430-cm^{-1} peak can then be ascribed to the sp^3 CH_2 scissors mode, since H is mainly bonded to sp^3 C sites as CH_2 (and CH) groups. It could also include some contribution from aromatic sp^2 CH bending modes, since series-I samples contain a non-negligible fraction of aromatic CH groups.

The well-defined band centered at 1580 cm^{-1}, which is observed in the series-I spectrum, must be ascribed to

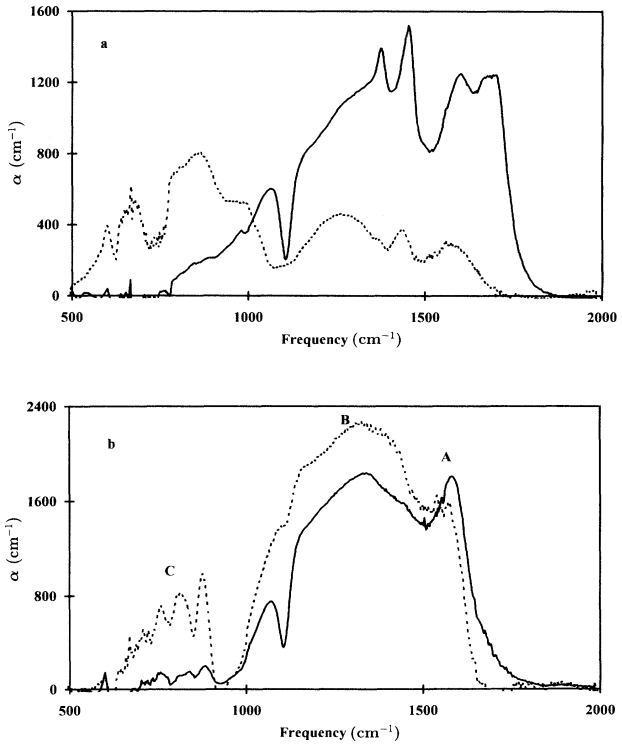

FIG. 6. Comparison of the low-frequency part of the IR absorption spectra of series I (dashed line) and series II (continuous line) samples: as-deposited (a) and annealed at $T_A = 600$ °C (b).

C=C double-bond stretching vibrations. The skeletal ring breathing modes of aromatic systems are for example found in this spectral range.[9,10,15] The width of this band suggests that the C=C bonds are found in many different configurations, both olefinic and aromatic (in agreement with the conclusions drawn from the C—H stretching band) and that these configurations are probably distorted. This can be related to the rigidity of the sp^3 C matrix connecting the π-bonded clusters, since this matrix contains little hydrogen. The broadening of the C=C band could also come from some interaction between the C=C vibrations and the adjoining sp^2 C—H vibrations. A peak centered at 1600 cm^{-1}, with a slight shoulder around 1560 cm^{-1}, is also seen in the series-II spectrum, and must have the same origin. It is unfortunately partially overlapped by the contamination band mentioned earlier, due to C=O (1700 cm^{-1}) and C=N (1670 cm^{-1}) stretching vibrations. The presence of an intense and sharp peak in this spectral range, characteristic of C=C double bonds, indicates that, although the proportion of sp^2 C atoms bonded to H is quite small (Table II), these samples contain an important fraction of sp^2 C atoms bonded to other C atoms only (i.e., not bonded to H). This is in agreement with the results of our previous electron-energy-loss spectroscopy studies.[3] The shift of this peak to higher frequencies with respect to that in series-I samples confirms the predominance of olefinic configurations in series-II samples.

If we now turn to lower energies, we observe a strong absorption just below (and partially overlapping) the sp^3 CH_x deformation vibration peaks. In series I, it appears as a broad maximum centered at about 1270 cm^{-1}, with a faint shoulder around 1170 cm^{-1}. In series II, where the contribution of the different sp^3 CH_x deformation vibrations is much more important because of a much larger concentration of bonded H, two corresponding features at about 1265 and 1170 cm^{-1} can be detected on the decreasing background. At this point, it is rather difficult to ascribe these features to particular vibrations, although olefinic sp^2 CH and sp^3 CH bending modes are expected around these frequencies.[2] According to the hydrocarbon studies, this band could also be due to C skeletal vibrations (mainly mixed sp^2/sp^3 modes)[6] enhanced by a more or less important coupling with CH group vibrations.[9,10]

As for the absorption that is still clearly observed below 1050 cm^{-1} in series I, but is practically absent in series II, it corresponds essentially to H bonded to sp^2 C sites, and confirms the difference between series I and series II in this respect. The sharp structures around 600–700 cm^{-1} suggest the presence of well-defined environments in series-I samples.

B. Annealing effects

In order to check our interpretation of the different structures in the IR absorption spectra over a wide frequency range, we have studied their modifications upon annealing at increasing temperatures T_A up to 600 °C, and we have analyzed the results in relation with the H evolution spectra discussed above, keeping in mind the differences in the kinetics of the two types of experiments. The IR data are summarized in Figs. 7(a), 7(b), and 8(a), 8(b) for the high- and low-frequency ranges, respectively.

1. Series I

For $T_A = 300$ °C, the part of the C—H stretching band corresponding to sp^3 CH_x groups is practically unchanged. The only modification of that band with respect to the as-deposited sample is an increase of the contribution of aromatic sp^2 CH groups ($\sim$3045 cm^{-1}) at the expenses of that of the olefinic sp^2 CH groups ($\sim$3000 cm^{-1}). This is in agreement with the very little loss of H (mainly as CH_4) below 400 °C in this series. The atomic rearrangements responsible for the increase of aromatic configurations are accompanied (Table I) by a small decrease of the film thickness d, the refractive index n_o remaining roughly the same. They could consist in the formation, for energetic reasons, of sp^2 C (H) cycles gathering into small isolated aromatic clusters, in regions where the sp^2 C (H) sites were initially organized in neighboring fragments of olefinic chains. This could explain the slight unexpected shift of the high-energy part of the optical-absorption edge and the appearance of a faint luminescence, as already reported.[3] Within our experimental accuracy, it is difficult to detect any change in the 1600-cm^{-1} region (ascribed to C=C stretching vi-

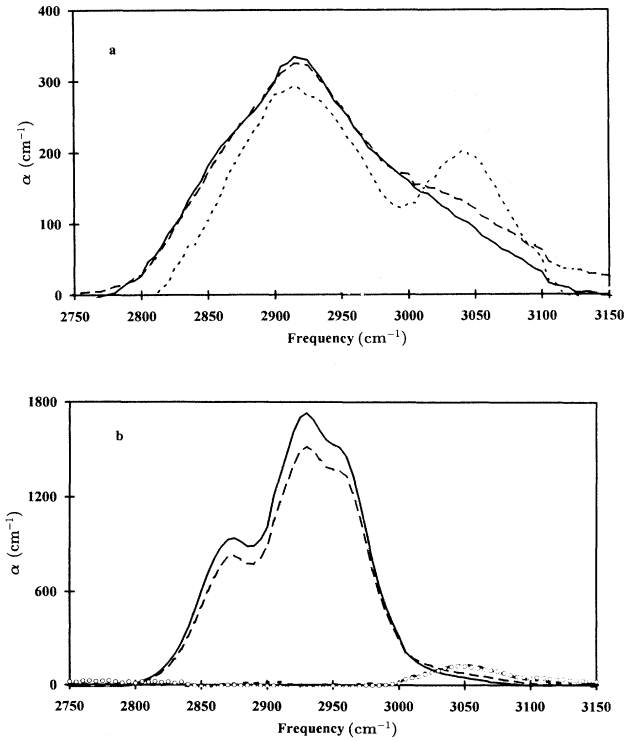

FIG. 7. Changes of the high-frequency C—H stretching bands of the IR absorption spectra of series I (a) and II (b) samples with annealing temperature T_A: as-deposited (continuous line); $T_A = 300$ (dashed line), 500 (dotted line), and 600 °C (empty circles).

brations), which could confirm this explanation.

For $T_A = 500\,^{\circ}C$, the C—H stretching band is strongly modified. It now practically reduces to two Gaussian components centered at ~ 2920 and 3045 cm^{-1}, respectively. The contributions of sp^3 CH_2 groups and of olefinic sp^2 CH_x groups seem to have almost completely disappeared, and H is then essentially bonded to sp^3 C sites as CH groups, and to sp^2 C sites as aromatic CH groups. At this annealing temperature, only a small amount of H has evolved from the film in the form of both H_2 and CH_4. It must be concluded that a significant proportion of sp^3 C sites bonded to H have been converted into sp^2 C sites without losing the bound H. The corresponding structural rearrangements are accompanied by a large decrease in d and increase in n_0 as well as by an important shift of the absorption edge to lower energies (Table I). Meaningful modifications are also observed in the IR absorption spectra at low frequencies. The broad maximum in the 1600-cm^{-1} range, indicating a large variety of C=C configurations, has changed into a well-defined and more intense peak centered at 1580 cm^{-1}. This suggests, not only an increase of the proportion of sp^2 C sites, but also a better organization of these sites into aromatic and/or graphitic clusters. The simultaneous increase and narrowing of the peak centered at ~ 1430 cm^{-1} is, on the other hand, in agreement with an increase of the concentration of aromatic sp^2 CH groups, and confirms our previous interpretation of the composite origin of this peak in the as-deposited films. It is worth noticing that the underlying wide absorption band is also significantly enhanced. A last annealing effect can be seen below 1100 cm^{-1}: the line shape of the spectrum is completely modified and sharp, well-defined structures can now be observed, especially the peaks at 880, 810, and 760 cm^{-1}. Such peaks are tentatively ascribed to rather localized deformation vibrations of aromatic CH groups.

For $T_A = 600\,^{\circ}C$, a temperature which corresponds to the maximum of the H evolution spectrum for both H_2 and CH_4, the stretching band corresponding to sp^3 CH_x groups has completely disappeared, while the subband ascribed to aromatic sp^2 CH groups at 3045 cm^{-1} has become more intense. This is the continuation of the process described for $T_A = 500\,^{\circ}C$, but now the strong departure of H has eliminated all sp^3 C sites bonded to H, an important proportion of these sites being transformed into sp^2 C sites without losing the bound H. In the low-frequency range, the IR spectrum reduces to an intense broad band from 1700 to 950 cm^{-1}, centered around 1350 cm^{-1} and exhibiting a well-marked shoulder (or peak ?) at about 1580 cm^{-1}, and to another band below 950 cm^{-1} presenting the same peaks as for $T_A = 500\,^{\circ}C$, but sharper and more intense. The whole IR absorption spectrum must then be dominated by the vibrations of the sp^2-bonded C skeleton, more or less strongly coupled with the vibrations of the remaining sp^2 CH groups.

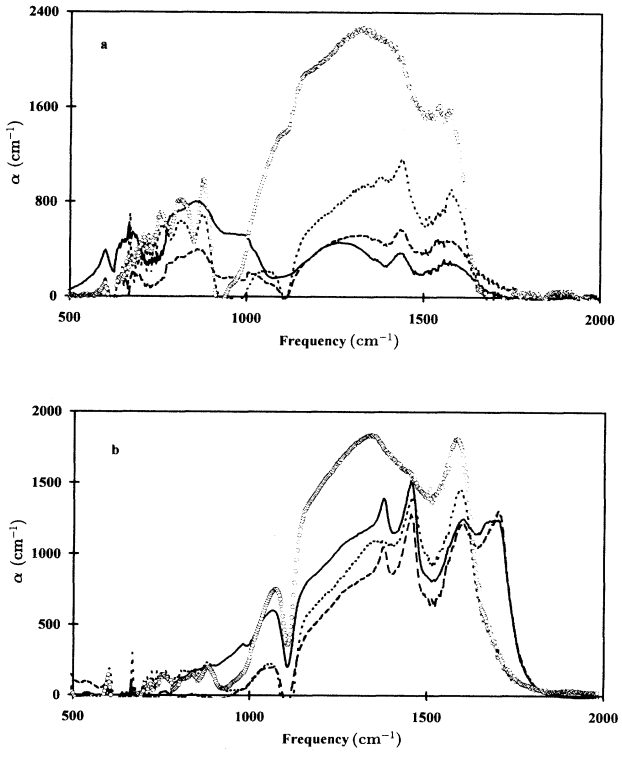

FIG. 8. Corresponding changes of the low-frequency part of the IR absorption spectra of series I (a) and II (b) samples with annealing temperature T_A: as-deposited (continuous line); $T_A = 300$ (dashed line), 500 (dotted line), and 600 °C (empty circles).

2. Series II

For $T_A = 300\,^{\circ}C$, the contributions of all the sp^3 CH_x groups to the C—H stretching band have already decreased, by about the same amount. This is consistent with the H evolution observed from 150–200 °C, mainly as CH_4 but also as H_2. The absorption due to the stretching vibrations of sp^2 CH_x groups, which is now easier to analyze due to the reduction of the OH contamination band, does not seem to have changed very much. In the low-frequency range, the only annealing effect is a decrease of the intensity of the doublet at 1455–1375 cm^{-1}, consistent with the decrease of sp^3 CH_3 groups. The peak at 1600 cm^{-1} attributed to C=C stretching vibrations remains exactly the same. Note that the C=N component of the contamination band overlapping this peak has disappeared, as well as the absorption between 800 and 900 cm^{-1}, which may also be due to contamination by ambient atmosphere. On the other hand, although a certain amount of bonded H has already left the sample, there is practically no variation either in d or in n_0 (Table I), which is at first sight rather surprising. However, there is simultaneously a large decrease of the optical gap, as well as a reduction of the photoluminescence intensity.[3] This indicates that the departure of CH_3 groups does change the connectivity of the C network even if it does not modify the film thickness. The resulting atomic rearrangements must favor the formation of larger π-bonded clusters and lower the barriers between these clusters coming from the "matrix."

For higher T_A, the gradual decrease of all the components of the C-H stretching band due to sp^3 CH_x groups continues, but is now accompanied by a decrease of d and an increase of n_0 (Table I). This is consistent with the steep rise observed in the H evolution spectrum, especially for CH_4 (and probably higher hydrocarbons). For $T_A = 500\,°C$, a temperature close to the maximum of the H evolution spectrum, all the sp^3 CH_x groups have completely disappeared and the C—H stretching band reduces to a faint single Gaussian centered at 3045 cm^{-1} (which had already emerged at $T_A = 400\,°C$). This shows that the remaining H atoms are only bonded to sp^2 C sites in aromatic configurations. There is, however, a difference with series I, since now only a very small proportion of the newly formed sp^2 C sites remains bonded to H. These conclusions are confirmed by the analysis of the low-frequency part of the IR absorption spectrum. The component of the doublet centered at 1375 cm^{-1} and attributed to sp^3 CH_3 groups has disappeared, while an intense peak can still be observed at 1450 cm^{-1}. This peak is then essentially ascribed to aromatic sp^2 CH bending modes. As for the peak in the 1600-cm^{-1} range, which can now be observed entirely due to the disappearing of the C=O contamination band, it is also very sharp and intense, and it has slightly shifted to lower frequencies. This indicates a large concentration of sp^2 C sites unbonded to H. Another striking feature is the appearance at $T_A = 500\,°C$ of an absorption band below 1100 cm^{-1} which, although less intense, resembles that seen for series I after annealing at the same T_A. For $T_A = 600\,°C$, the peak at 1450 cm^{-1} merges into a wide absorption band again very similar to that observed in series I for the same T_A, while the C=C peak, which is now centered at 1580 cm^{-1}, remains very intense.

The striking similarity between the samples of the two series after annealing at $T_A = 600\,°C$ is emphasized in Fig. 6(b). The same features are observed in both cases: a strong peak or pronounced shoulder centered at 1580 cm^{-1} corresponding to localized stretching vibrations of the C=C double bond in aromatic and/or graphitic configurations (A), a wide band centered at about 1350 cm^{-1} with very similar shape (B), and sharp peaks at well-defined identical frequencies below 900 cm^{-1} (C). The lower intensity of part (C) in series II is ascribed to the lower bonded H content. The remaining H atoms are certainly very strongly bonded to aromatic sp^2 C sites in both cases, since they start to evolve as H_2 at quite high temperatures ($> 600\,°C$, even $> 700\,°C$ in series I).

The IR absorption peak centered at 1580 cm^{-1} is strongly reminiscent of the main sharp "graphitic" peak observed at the same frequency in the Raman spectra of the annealed samples ($T_A = 600\,°C$),[3] as already noticed.[15] As for the wide IR absorption band centered at 1350 cm^{-1}, it is tempting to compare it to the low-frequency broader component of the same Raman spectra, peaking at about 1360 cm^{-1}.[3] Although the IR data probably still include contributions from C—H vibrations, this similarity suggests that, at least for films annealed at high temperature, the IR and Raman features may have a common origin.

V. CONCLUSION

The comparison of the results of several complementary experiments performed as a function of annealing on two series of a-C:H films prepared under quite different conditions illustrates the complexity of the role of hydrogen on the a-C:H microstructure. In particular, a careful analysis of the IR vibrational absorption spectra over a wide frequency range down to 500 cm^{-1} allows us to follow the changes in both C—H and C—C configurations upon annealing. Our work confirms that the bonded H concentration or the respective proportions of sp^2 and sp^3 C sites are not the pertinent parameters for understanding the relations between the electronic properties and the microstructure. The preferential attachment of H to sp^2 or sp^3 C sites as well as the variations in the C skeleton morphology when changing the deposition conditions has been clearly demonstrated. In particular, the π-bonded configurations seem to be more distorted in our hard, small gap samples, probably due to the stiffness of the sp^3 C matrix containing little hydrogen. In addition, we have shown that, if the breaking of sp^3 C—H bonds upon annealing tends to favor the transformation of these C sites into sp^2 C sites, as commonly admitted, these newly created π-bonded C atoms may either remain bonded to H (in diamondlike films) or be linked to other C atoms only (in polymerlike films). These different behaviors are correlated with the initial sample microstructure, and correspond to different processes in H evolution. Another important result is that samples having initially quite different morphologies tend to exhibit very similar IR absorption and Raman spectra after annealing at high enough temperature (600 °C in our case), even if they still retain different bonded H contents and different optical gaps.

ACKNOWLEDGMENTS

The authors are indebted to J. C. Pesant, from Laboratoire de Physique des Solides, CNRS-Bellevue, for his help with the hydrogen evolution experiments and to Dr. J. M. Frigerio for providing us with the procedure of interference fringe elimination in the IR data.

[1] J. Robertson, Adv. Phys. **35**, 317 (1986).
[2] J. Robertson, Prog. Solid State Chem. **21**, 199 (1991).
[3] Y. Bounouh, M. L. Thèye, A. Dehbi-Alaoui, A. Matthews, J. Cernogora, J. L. Fave, C. Colliex, A. Gheorghiu, and C. Sénémaud, Diamond Rel. Mater. **2**, 259 (1993).
[4] Ch. Wild and P. Koidl, Appl. Phys. Lett. **51**, 1506 (1987).
[5] X. Jiang, W. Beyer, and K. Reichelt, J. Appl. Phys. **68**, 1378 (1990).
[6] P. Koidl, Ch. Wild, B. Dischler, J. Wagner, and M. Ramsteiner, Mater. Sci. Forum **52-53**, 41 (1989).

[7]P. J. R. Honeybone, R. J. Newport, W. S. Howells, J. Tomkinson, and P. J. Revell, Chem. Phys. Lett. **180**, 145 (1991).
[8]B. Dischler, A. Bubenzer, and P. Koidl, Solid State Commun. **48**, 105 (1983).
[9]L. J. Bellamy, *The Infrared Spectra of Complex Molecules* (Chapman and Hall, London, 1975).
[10]N. B. Colthup, L. H. Daly, and S. E. Wiberley, *Introduction to Infra-red and Raman Spectroscopy* (Academic, London, 1990).
[11]B. Dischler, A. Bubenzer, and P. Koidl, Appl. Phys. Lett. **42**, 636 (1983).
[12]D. R. McKenzie, R. C. McPhedran, N. Savvides, and L. C. Botten, Philos. Mag. B **48**, 341 (1983).
[13]M. P. Nadler, T. M. Donovan, and A. K. Green, Thin Solid Films **116**, 241 (1984).
[14]R. Memming, Thin Solid Films **143**, 279 (1986).
[15]M. A. Tamor, C. H. Wu, R. O. Carter III, and N. E. Lindsay, Appl. Phys. Lett. **55**, 1388 (1989).
[16]J. Gonzalez-Hernandez, B. S. Chao, and D. A. Pawlik, J. Vac. Sci. Technol. A **7**, 2332 (1989).
[17]J. H. Kaufman, S. Metin, and D. D. Saperstein, Phys. Rev. B **39**, 13 053 (1989).
[18]O. Stenzel, G. Schaarschmidt, F. Wolf, M. Vogel, and T. Wallendorf, Thin Solid Films **203**, 11 (1991).
[19]A. Grill and V. Patel, Appl. Phys. Lett. **60**, 2089 (1992).
[20]J. Biener, A. Schenk, B. Winter, C. Lutterloh, U. A. Schubert, and J. Küppers, Surf. Sci. Lett. **291**, L725 (1993).